Acta Cryst. (1982). A**38**, 710–717

Determination of the Position of Even the Lighter Anomalous Scatterers in a Crystal Structure by means of a Two-Wavelength Technique*

BY G. CASCARANO AND C. GIACOVAZZO

Istituto di Mineralogia, Università Palazzo Ateneo, 7021, Bari, Italy

AND A. F. PEERDEMAN† AND J. KROON

Laboratorium voor Structuurchemie, Rijksuniversiteit Padualaan 8, Utrecht, The Netherlands

(*Received* 3 *August* 1981; *accepted* 22 *April* 1982)

Abstract

For identical anomalous scatterers among a majority of normal scatterers the structure-factor amplitudes are estimated from intensity data obtained either with two wavelengths at one side of the absorption edge or with one wavelength at either side. Direct methods (or a Patterson synthesis) will allow the localization of these anomalous scatterers. Test calculations on the known structure of the iron-containing protein ferredoxin, simulating the effects of synchrotron radiation, show the feasibility of the procedure.

1. Introduction

The advent of synchrotron radiation as a tunable source for X-ray diffraction experiments has opened new prospects for the application of anomalous diffraction in crystal-structure determination, and particularly for the X-ray analysis of proteins. If conventional X-ray sources with their characteristic wavelengths are used one usually has to resort to the introduction of heavier atoms in the protein structure in order to secure the event of non-negligible anomalous-dispersion effects. This, however, is quite often accompanied by preparative troubles, deviation from isomorphism with the native compound and as a rule non-stoichiometric occupancy by the heavy atoms introduced. By virtue of the tunability of synchrotron radiation, one can get nearer to an absorption edge so that even for not-so-heavy atoms – which are frequently present in natural proteins (*e.g.* Fe and S) – the anomalous component of the scattering factor becomes rather large. Thus, by variation of the wavelength fairly great changes can be attained in the real as well as in the imaginary part of the anomalous component.

In this paper we will show that, solely from the changes in diffraction intensities, it is possible in practice to estimate the structure-factor amplitudes of the anomalous scatterers. A Patterson synthesis based on these values will produce only the vectors between the anomalous scatterers. In our example we determined the arrangement of the Fe atoms by application of direct methods to the estimated contributions of these anomalous scatterers.

One application of the observed anomalous scattering for the determination of the positions of the anomalous scatterers has been described by Rossmann (1961). In his one-wavelength approach it is shown that a Patterson synthesis with $\{|F(\mathbf{h})| - |F(\bar{\mathbf{h}})|\}^2$ coefficients will produce peaks at the ends of vectors that relate anomalous scatterers.

In the past several authors have already stressed the usefulness of two-wavelength experiments.

Ramaseshan (1966) introduced an addition-Patterson synthesis with neutron diffraction data using coefficients $|F(\mathbf{h})_{\lambda_1}|^2 + |F(\mathbf{h})_{\lambda_2}|^2$ (λ_1 and λ_2 on either side of the resonance wavelength), in which vectors between anomalous scatterers and normal scatterers can be suppressed by a proper choice of wavelengths.

Bartunik (1978) proposed a new two-wavelength Bijvoet-pair method which allows unique determination of phases. His method requires that the resonant-atom structure is known and that the real and imaginary components obey certain conditions. It has the great advantage that absorption corrections need not be carried out. The use of the ratio of the intensities of Bijvoet pairs instead of Bijvoet differences has been advocated by Unangst and co-workers (Unangst, Müller, Müller & Keinert, 1967). In the same paper they also point out the possibility of gaining information about the contribution of the anomalous scatterers by measuring intensities at two or more wavelengths *within* the anomalous-dispersion region. Hoppe & Jakubowski (1975) suggest the use of a parameter-shift procedure in which the anomalous-scatterer configuration is determined from two-wave-

* Presented at the Sixth European Crystallographic Meeting, Barcelona, Spain, 28 July–1 August 1980. Abstract 2A-17.

† To whom correspondence should be addressed.

0567-7394/82/050710-08$01.00

length data. Finally Karle (1980) in his calculations completely separates the anomalous from the normal scattering and obtains linear equations from which the values of the anomalous-scatterer contributions are to be evaluated.

In the present paper we will give *explicit* expressions for the contributions of the anomalous scatterers in terms of measurable quantities in a two-wavelength experiment, which is supposed to be carried out with either both wavelengths at one side of the absorption edge or one wavelength at either side. The theory is restricted to the case of only one type of anomalous scatterer, but may be extended to more types of anomalous scatterers and more wavelengths.

Our approach resembles that of Singh & Ramaseshan (1968), who, however, tacitly assume the experimental data to be on an absolute scale. This leads to expressions for the anomalous-scatterer contribution that differ from our final formulae. Furthermore, it must be noted that their equations (5) and (6) are multiplied by the real components of the anomalous parts of the scattering factors at two wavelengths. This implies that their results only apply to an experiment carried out with both wavelengths at the high-frequency side of the absorption edge.

2. Definitions and abbreviations

p, q	number of anomalous and non-anomalous scatterers respectively in the unit cell
n	number of atoms in the unit cell ($n = p + q$)
f^0	high-frequency limit of the atomic scattering factor
f', f''	real and imaginary dispersion corrections for the atomic scattering factor
$f = f^0 + f' + if''$	general expression for the atomic scattering factor
$\mathbf{F}^0$	structure factor (imaginary component of anomalous dispersion omitted)
$\mathbf{F}_j^+$	structure factor of reflection $\mathbf{h}$ for wavelength $\lambda_j; j = 1, 2$
$\mathbf{F}_j^-$	structure factor of reflection $-\mathbf{h}$ for wavelength $\lambda_j; j = 1, 2$
$\mathbf{F}'_p$	contribution of anomalous scatterers [only real component of anomalous diffusion (f') included]
$\mathbf{F}''_p$	contribution of anomalous scatterers due to imaginary component of anomalous diffusion

$$\mathbf{F}''_p = f'' \sum_{j=1}^{p} \exp 2\pi i \mathbf{h}\mathbf{r}_j$$

$\mathbf{g}$	the contribution of the anomalous scatterers with their scattering factor equal to unity

$$\mathbf{g} = \sum_{j=1}^{p} T_j \exp 2\pi i \mathbf{h}\mathbf{r}_j$$

(T_j is the temperature factor)

$F^0, F^+, \ldots, g$	moduli of $\mathbf{F}^0, \mathbf{F}^+, \ldots, \mathbf{g}$ respectively
f'_1	f'_{λ_1} *etc.*
Δ	$\lvert f'_1 - f'_2 \rvert$
v_j	$v_j \equiv (F_j^+)^2/(F_j^-)^2; j = 1, 2$
s_j	$s_j \equiv f''_j(v_j + 1)/(v_j - 1); j = 1, 2$
t	$t \equiv (F_1^0)^2/[(F_2^+)^2 - (F_2^-)^2]$
T	$T \equiv 1/t$
X	$X \equiv 2[(F^+)^2 - (F^-)^2]/[(F^+)^2 + (F^-)^2] = 2f''/s$
κ	$\kappa \equiv f''/[f^0 + f']$

$$\sigma_1 \equiv \frac{\left[\sum_{j=1}^{p} (f_j^0 + f_j')^2\right]}{\left[\sum_{j=1}^{n} (f_j^0 + f_j')^2\right]}$$

$$\sigma_2 \equiv \left[\sum_{j=1}^{q} (f_j^0)^2\right] \Big/ \left[\sum_{j=1}^{n} (f_j^0 + f_j')^2\right]$$

c.s.	centrosymmetrical
n.c.s.	noncentrosymmetrical

3. Geometrical approach

The procedure is based on the Argand diagrams in Fig. 1, and aims at the calculation of the ratios between F^+, F^- and F'' from two-wavelength experimental data. This ratio is obtained for each of all the Bijvoet pairs separately. After this the F'' values of all individual Bijvoet pairs are scaled relative to each other by observing the common scale of the intensity data. Finally, the squares of F'' can be used as Patterson coefficients. The resulting map should have the characteristics of a sharpened Patterson map of the anomalous scatterers only, because F'' contains the same geometrical factor as the normal contribution to the structure factor, and the 'scattering factor' f'' changes very little with the scattering angle. A plausible alternative to the Patterson analysis is the application of direct methods.

The geometrical solution of the first part of the procedure is shown in Fig. 2, where $AO = OB$ represents for wavelength λ_1 the length of F''_1 on some arbitrary scale. We now consider a triangle for which $AP/BP = F_1^+/F_1^-$. This ratio then fixes the points D ($AD/DB = F_1^+/F_1^-$) and D' ($AD'/BD' = F_1^+/F_1^-$), where inner and outer bisectors of the top angle P intersect the base of the triangle. As these bisectors are mutually

perpendicular they restrict the position of the top P to the points on the circle M with DD' as a diameter.

If the second wavelength λ_2 is at the same side of the absorption edge as λ_1 we add to Fig. 2 O_1O_2 and $A_2O_2 = O_2B_2$ representing $\Delta = g|F_2' - F_1'|$ and F_2'' respectively (Fig. 3). This is possible because $F_1'':|F_2' - F_1'|:F_2'' = f_1'':|f_2' - f_1'|:f_2''$, of which f_1', f_1'', f_2' and f_2'' are known.

The ratio F_2^+/F_2^- for the second wavelength allows a similar circle to that in the case of λ_1. The intersection of the two circles in this bianomalous case yields two possible solutions for P and thus for the ratio between F'' and any observable quantity like, for example, F_1^+. When the ratio F_2^+/F_2^- is either close to unity, or exactly equal to unity, as in the monoanomalous case ($f_2'' = 0$), the ratio F_2/F_1^+ must provide for the second circle. This, however, requires the experimental intensities for the two wavelengths to be on the same scale. In the bianomalous case this condition may serve as a means of discriminating between the two solutions obtained. In both cases the discrimination can be accomplished by means of statistical considerations. It may happen that

(*a*) for c.s. and pseudo-centrosymmetrical reflections the phases of the normal contribution of the anomalous scatterers and the contribution of the other atoms are equal or differ by π. This case results in equal ratios $F^+/F^- = 1$ for both wavelengths; the intensities, however, are different for the two wavelengths. The resulting difference in F yields Δg and consequently F'' by virtue of its constant ratio to Δg.

(*b*) the contribution of the anomalous scatterers to the structure factor is zero, resulting in four equal intensities for the Bijvoet pair, regardless of the two wavelengths. As these reflections do not contain an F'' they are irrelevant for our purpose.

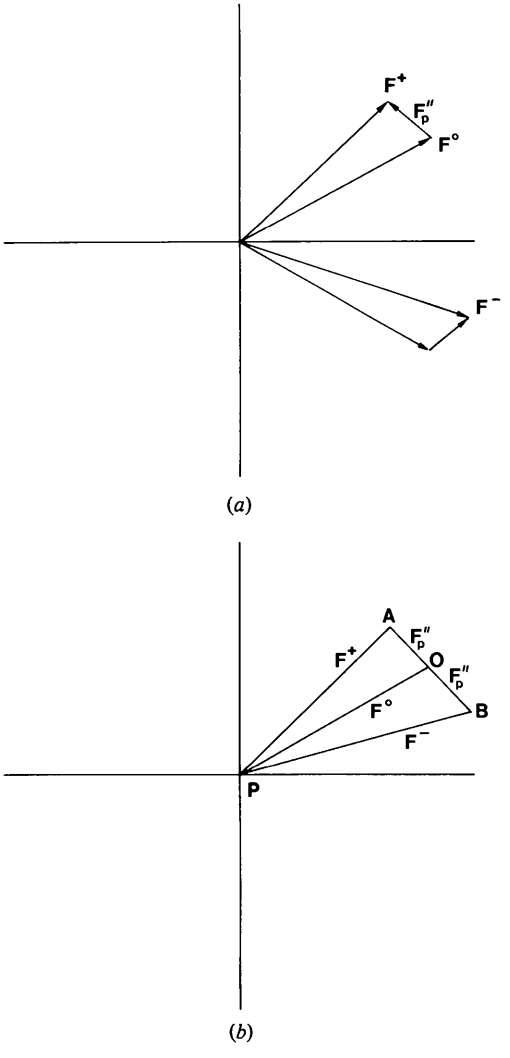

Fig. 1. (*a*) Argand diagram in the case of anomalous scattering (for symbols see text); (*b*) Same diagram as in (*a*), but with the lower triangle reflected in the real axis.

4. Algebraic calculations

In this section we derive the algebraic expressions for g in accordance with the geometrical approach described in § 3. We will also show that the procedure may be used for estimating g when the reflection is c.s.

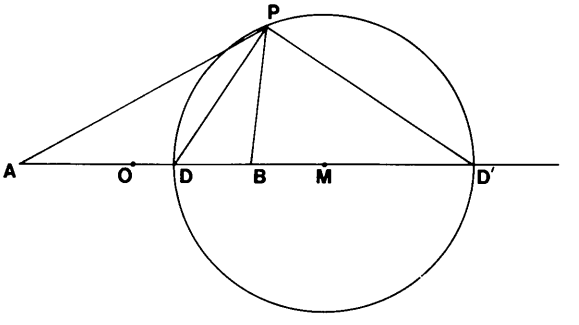

Fig. 2. Construction of the locus of points P for which $PA/PB = F^+/F^-$.

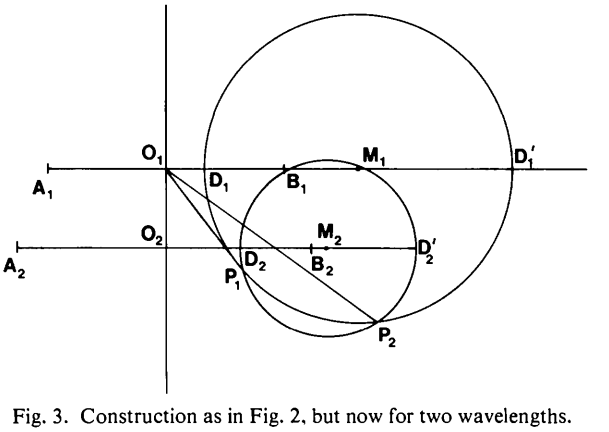

Fig. 3. Construction as in Fig. 2, but now for two wavelengths.

Bianomalous case ($f_1'' \neq 0; f_2'' \neq 0$)

Given the values of f_1', f_2', f_1'', f_2'', v_1 and v_2 the problem that faces us is to find the coordinates x and y of the points P for which $PA_1/PB_1 = F_1^+/F_1^-$ and $PA_2/PB_2 = F_2^+/F_2^-$. We have to solve the equations

$$[(gf_1'' + x)^2 + y^2]/[(gf_1'' - x)^2 + y^2] = v_1, \quad (1)$$

$$[(gf_2'' + x)^2 + (y - g\Delta)^2]/[(gf_2'' - x)^2 + (y - g\Delta)^2] = v_2. \quad (2)$$

We may rewrite (1) and (2) in the form

$$x^2 + y^2 - 2gs_1 x + g^2 f_1''^2 = 0 \quad (3)$$

$$x^2 + y^2 - 2gs_2 x - 2g\Delta y + g^2(f_2''^2 + \Delta^2) = 0. \quad (4)$$

Intersections of the corresponding circles give the solutions for x and y as a function of g; in Fig. 4 an 'experimental' example is given. We get for the two solutions P_1 and P_2

$$x_\pm = gQ_\pm$$

where

$$Q_\pm = \frac{1}{2[\Delta^2 + (s_1 - s_2)^2]}\{(f_1''^2 - f_2''^2)(s_1 - s_2) + \Delta^2(s_1 + s_2) \pm \Delta]4s_1 s_2(f_1''^2 + f_2''^2 + \Delta^2) - 4(s_1^2 f_2''^2 + s_2^2 f_1''^2) - (f_1''^2 - f_2''^2 - \Delta^2)^2 - 4\Delta^2 f_1''^2]^{1/2}\} \quad (5)$$

and

$$y_\pm^2 = gR_\pm^2,$$

where

$$R_\pm^2 = 2s_1 Q_\pm - f_1''^2 - Q_\pm^2. \quad (6)$$

Next g can be determined by (7) if F_1^0 is known:

$$x_\pm^2 + y_\pm^2 = g^2(Q_\pm^2 + R_\pm^2) = (F_1^0)^2. \quad (7)$$

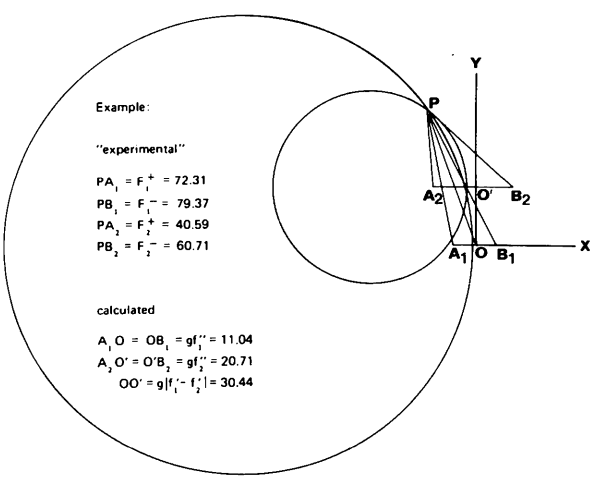

Fig. 4. Practical example in the bianomalous case.

In practice F_1^0 is unknown and discrimination between the two solutions g_+ and g_- is needed. We will show in § 5 how these difficulties can be satisfactorily overcome. Here we only note that $g^+ \equiv g^-$ when $Q^+ \equiv Q^-$.

If the reflection is c.s. (then $F_1^+ = F_1^- \equiv F_1$, $F_2^+ = F_2^- \equiv F_2$), the point P in Fig. 4 must lie on the y axis so that the ratios PA_1/PB_1 and PA_2/PB_2 equal unity. Then g may be estimated *via* the equation

$$PA_1^2/PA_2^2 = [g^2 f_1''^2 + y^2]/[g^2 f_2''^2 + (y - g\Delta)^2] = F_1^2/F_2^2$$

which leads to

$$y^2(F_2^2 - F_1^2) + 2g\Delta F_1^2 y + g^2[f_1''^2 F_2^2 - (f_2''^2 + \Delta^2)F_1^2] = 0$$

from which

$$y_\pm = g\frac{\left\{\begin{matrix}-\Delta F_1^2 \pm [F_1^2 F_2^2(f_1''^2 + f_2''^2 + \Delta^2) \\ - F_1^4 f_2''^2 - F_2^4 f_1''^2]^{1/2}\end{matrix}\right\}}{F_2^2 - F_1^2} = gT_\pm. \quad (8)$$

Next g may be determined by (9) if F_1^0 is known:

$$(y_\pm)^2 = g^2(T_\pm)^2 = (F_1^0)^2. \quad (9)$$

As for (7), F_1^0 is unknown in practice and discrimination between the two solutions g_+ and g_- is needed. The reader is again referred to § 5.

Monoanomalous case ($f_1'' = 0, f_2'' \neq 0$)

Given the values of f_1', f_2', f_1'' ($\equiv 0$), f_2'', t and v_2, the problem that faces us is to find the coordinates x and y of the points P for which

$$PA_2/PB_2 = F_2^+/F_2^-$$

and

$$\frac{PA_2^2 - PB_2^2}{PO_1^2} = \frac{(F_2^+)^2 - (F_2^-)^2}{(F_1^0)^2}.$$

We have to solve the system of equations (2) and (10):

$$T = 4gf_2'' x/[x^2 + y^2]. \quad (10)$$

Equation (10) may be written as $x^2 + y^2 - 4gtf_2'' x = 0$, which is the equation of a circle. Intersection of the circles corresponding to (2) and (10) give the solutions for x and y as a function of g. For the two solutions P_1 and P_2 we get

$$x_\pm = g\frac{-b \pm \{b^2 - [c^2 + \Delta^2][f_2''^2 + \Delta^2]^2\}^{1/2}}{2[c^2 + \Delta^2]} = gQ_\pm, \quad (11)$$

where

$$b \equiv c(f_2''^2 + \Delta^2) - 4\Delta^2 f_2' t,$$
$$c \equiv (2f_2'' t - s_2)$$

and

$$y_\pm^2 = g^2(4tf_2'' Q_\pm - Q_\pm^2) = g^2 R_\pm^2. \quad (12)$$

Since

$$x_{\pm}^2 + y_{\pm}^2 = g^2\{Q_{\pm}^2 + R_{\pm}^2\} = (F_1^0)^2 \qquad (13)$$

two solutions for g arise from (13):

$$(g_{\pm})^2 = (F_1^0)^2/(Q_{\pm}^2 + R_{\pm}^2). \qquad (14)$$

F_1^0 is now a measured quantity. Therefore we have only to discriminate between g_+ and g_-. An 'experimental' example is given in Fig. 5.

If the reflection is c.s. (then $F_2^+ = F_2^- \equiv F_2$ and $F_1^0 \equiv F_1$) the point P lies on the y axis so that PA_2/PB_2 equals unity. Then g may be estimated *via* the equation

$$\frac{PA_2^2}{PO^2} = \frac{g^2 f_2''^2 + (y - \Delta g)^2}{y^2} = \frac{F_2^2}{F_1^2}$$

from which

$$y_{\pm} = g\,\frac{\Delta F_1^2 \pm F_1[f_2''^2(F_2^2 - F_1^2) + F_2^2\Delta^2]^{1/2}}{(F_1^2 - F_2^2)} = gT_{\pm}. \qquad (15)$$

Next g may be estimated by (16):

$$(y_{\pm})^2 = g^2(T_{\pm})^2 = F_1^2 \qquad (16)$$

which gives two solutions again, g_+ and g_-.

5. Practical considerations

The application of the algebraic procedure described in § 4 requires that two conditions are satisfied: (*a*) the equations estimating $g_{\pm}$ should not be too sensitive to experimental errors. In other words, small errors in measurements of parameters involved in the equations should not give rise to prohibitive errors in g; (*b*) practical discrimination between g_+ and g_- should be correct for a sufficiently large number of reflections.

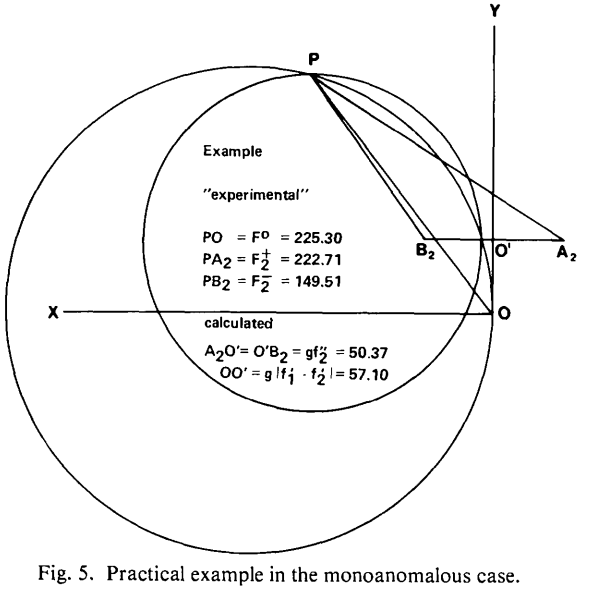

Fig. 5. Practical example in the monoanomalous case.

As for (*a*) it should be observed that diffraction observations are always and simultaneously affected by both systematic and random errors, although to a different extent. Typical error sources are the non-uniform film sensitivity in photographic techniques or counting errors in counting devices, occurrence of multiple scattering, absorption corrections (their change with wavelength must be taken into account), extinction *etc.* Hoppe & Jakubowski (1975) carefully analyzed the effect of the most important error sources on the success or failure of a two-wavelength method. They found that when the anomalous difference is of the order of 2% success may be expected if the intensities are measured with an accuracy of 10% (corresponding to a structure-factor accuracy of 5%) and if the relative accuracy of F^+ and F^- is good enough (less than 0·25%). Such performance may frequently be obtained if measuring techniques are used which aim at accurate measurements of intensity differences instead of intensities themselves. For example, intensities should be measured in 'pairs' in counter experiments so that radiation damage will influence all measurements in the same way. A consequence is that the observed values of F^+ and F^- are likely to be on the same (but unknown) scale. Since only the ratios F^+/F^- are involved in (5) and (6) for the estimation of $Q_{\pm}$ and $R_{\pm}$ in the bianomalous case it is sufficient that F^+ and F^- are on the same scale. If the experimental conditions comply with the monoanomalous case then the relative scale factors of the observations at the two wavelengths are also needed [in view of t in (11) and (12)]. Treatment of c.s. reflections [see (8) and (15)] always requires the relative scaling of observations at the two wavelengths. This is not an insuperable problem if an optimized scheme is used which measures each batch of reflections at the different wavelengths consecutively. In any case the well known schemes for the relative scaling of the isomorphous derivatives of proteins can be used for the anomalous data too.

It seems reasonable to suppose that when the anomalous difference exceeds 2% (which frequently occurs when synchrotron radiation is used) the above requirements on the absolute and on the relative accuracy of the structure factors can be relaxed even more. The anomalous difference can be estimated *a priori* by calculating the probability distribution function of the Bijvoet ratio X, for the actual cell contents and the wavelength chosen. Theoretical expressions of the expectation values of X were derived by Parthasarathy (1967) for n.c.s. crystals in which the anomalous scatterers are identical. When many identical anomalous scatterers are present, which are uniformly distributed in the cell, then

$$\langle X \rangle = 4\kappa\sigma_1\,\sigma_2. \qquad (17)$$

Thus $\langle X \rangle$ is seen to depend on both κ and σ. When synchrotron radiation is used strong changes in the real

and imaginary components of the anomalous scattering factor of many atoms can be obtained if the wavelength of the X-ray beam is suitably tuned around the K or L absorption edge. For example, the scattering amplitude of cesium is reduced by as much as 25 electrons per atom when synchrotron radiation near the L_{III} absorption edge is used (Phillips, Templeton, Templeton & Hodgson, 1978). An f' value of about -10 and an f'' value of about $+6$ e can be obtained for Fe by tuning the wavelength around its K edge (Phillips *et al.*, 1977). That gives $\kappa \simeq 0{\cdot}35$ at $\sin\theta/\lambda = 0$; higher values of κ occur when $\sin\theta/\lambda$ increases because of the fact that f^0 decreases when $\sin\theta/\lambda$ increases whereas f'' is very nearly independent of $\sin\theta/\lambda$ (Matthews, 1966). Such conditions appear to be very favourable for minimizing the effects of notable errors in measurements or in their subsequent treatment and to preserve high resolution of the g^2 Fourier syntheses.

As for point (*b*), g_+ and g_-, as obtained by application of (7), (9), (14), and (16), will be on the same relative scale as the diffraction data. This situation has no disturbing effect, neither on a Patterson synthesis nor on the application of direct methods, provided we are able to choose correctly between g_+ and g_-. The discrimination can be made in most cases by statistical methods, requiring:

(i) The application of suitable distribution laws for X-ray intensities. Depending on the value of p, pertinent distributions (Parthasarathy & Srinivasan, 1964) must be applied in order to estimate the most probable value of g.

(ii) The observed structure factors are on an absolute scale. Scaling errors of 5–10% occur frequently when statistical methods are applied. However, because of (i), errors of such a magnitude can hardly impair the results of the procedure.

As for the discrimination between g^+ and g^- in our calculations we will always choose the minimum as the 'best' g. Such a choice is in agreement with the probability laws of the normalized intensities (Wilson, 1949), but an assessment of its general effectiveness requires some more tests. This discrimination *via* the minimum value resembles that between the two values for the heavy-atom contribution that are derived from isomorphous and anomalous differences as done by Dodson & Vijayan (1971).

6. Practical applications

To gain an insight in the feasibility of the procedure we tested the influence of experimental errors by simulating experimental conditions and using calculated structure factors. We choose the ferredoxin from *Peptococcus aerogenes* (Sieker, Adman & Jensen, 1972) which crystallizes in $P2_12_12_1$ with $a = 30{\cdot}52$, $b = 37{\cdot}75$ and $c = 39{\cdot}37$ Å and $M_r \simeq 6000$. There are eight iron atoms in the molecule. The regions of outstanding electron density are those occupied by two cube-like clusters with Fe atoms at four alternate corners in a tetrahedral fashion and S atoms at the other four corners. In spite of the relatively large Bijvoet differences with Cu $K\alpha$ radiation, attempts of Sieker *et al.* (1972) to locate the Fe atoms by the Patterson synthesis with $(|F^+| - |F^-|)^2$ as coefficients failed because of the noise in the map and the complexity of the Fe–S clusters. The structure was solved by Adman, Sieker & Jensen (1973) by means of the heavy-atom derivatives. The pseudo-experimental conditions we chose are shown in Table 1. The values of $\langle|X|\rangle$ from experimental data are 0·39 for $\lambda = 1{\cdot}743$ Å amd 0·20 for $\lambda = 1{\cdot}541$ Å.

Table 1. *Pseudo-experimental conditions*

(i) Synchrotron radiation.
(ii) Calculated structure factors [B(overall) = 10 Å^2].
(iii) Experimental errors simulated by assignment of random errors.

Fe	λ_1 (Å)	λ_2 (Å)	f'_1	f'_2	f''_1	f''_2
Bianomalous	1·541	1·743	−1·18	−10·00	3·20	6·00
Monoanomalous	1·789	1·743	−3·20	−10·00	0	6·00
Resolution 2 Å						
Number of reflections	3328					

We made the calculations on the basis of the following criteria:

(*a*) If F_1^+/F_1^-, F_2^+/F_2^- and F_1^+/F_2^+ are simultaneously close to unity then the reflection is not processed. This situation corresponds to reflections for which $g \simeq 0$, which are of minor importance. In practice we only considered the reflections for which $|\text{ratio} - 1| \geq 0{\cdot}05$. Because of the value of $\langle X\rangle$ this condition is not too severe: less than 10% of the reflections were left out. Anyway we exclude from further calculations reflections for which the value of g_+ or g_- is smaller than 3 (about 25% of the reflections can be expected to satisfy this condition).

(*b*) If $F_1^+/F_1^- \simeq 1$ and $F_2^+/F_2^- \simeq 1$ but F_1^+/F_2^+ or $F_1^-/F_2^- \neq 1$, then the reflection is processed as if it were centrosymmetrical (pseudo-symmetrical reflections in Tables 3, 4 and 5). This procedure aims at the minimization of the effects of the experimental errors on the calculated value of g.

(*c*) If, because of errors, the square-roots occurring in the expressions of $Q_\pm$, $R_\pm$ and $T_\pm$ become imaginary then they are put equal to zero.

Inherent to the method is that F_1^0 is not exactly known in the bianomalous case. However, in most cases (Petsko, 1976),

$$F_1^0 \simeq \tfrac{1}{2}(F_1^+ + F_1^-), \tag{18}$$

which is used by us as an approximation. Sometimes (18) is too rough and its application leads to a bad estimation of g. The use of the algebraic relation

$$(F_1^0)^2 = \tfrac{1}{2}[(F_1^+)^2 + (F_1^-)^2] - g^2 f_1''^2 \tag{19}$$

allows us to find out the reflections for which (18) does not hold. We only compare the values of F_1^0 arising

from (18) and (19): if they differ by more than 15% we do not use the reflection, otherwise the F_1^0 value given by (19) is used as a refined value for calculating g.

Practical tests were made (i) without introducing and (ii) by introducing errors in the data. In case (ii) random errors normally distributed with $\sigma = 0{\cdot}01$, $0{\cdot}02$ and $0{\cdot}04$ are independently applied to each structure factor. Since structure factors enter in the algebraic equations *via* the parameters X for the bianomalous and T for the monoanomalous case, the errors modify their numerical values. In order to judge the stability of the method we give in Table 2 the average values $\langle |X - Xe| \rangle$ and $\langle |T - Te| \rangle$ for different wavelengths, where X, T, Xe, Te symbolize the values of X and T without and with error.

In Tables 3 and 4 we give, for the bianomalous and the monoanomalous case, respectively, the number of reflections used in the calculations for each chosen standard deviation σ of the error and the following two R indices:

$$R_{F_0} \equiv \sum |F_1^0 - [0{\cdot}5(F_1^+ + F_1^-)]| / \sum F_1^0$$

$$R_g \equiv \sum |g_{\text{true}} - g_{\min}| / \sum g_{\text{true}}.$$

The entries refer to different families of reflections.

The tables suggest: (1) equation (18) is a quite good approximation for practical purposes even when the error is relatively large; (2) the method works in the monoanomalous case with about the same accuracy for the different families of reflections; (3) as an effect of the increasing error, the accuracy of the method in the bianomalous case is higher for the pseudocentrosymmetric than for the non-centrosymmetric reflections. This encouraged us to treat suitable non-centrosymmetric as pseudo-centrosymmetric reflections. In Table 5 the outcome is shown when the reflections for which [see conditions (*a*) and (*b*) in § 5] $|\text{ratio} - 1| \leq 0{\cdot}10$ are considered pseudo-centrosymmetric. The new procedure caused a notable improvement in the R_g index, which makes the method practicable even in the case of relatively large experimental errors.

The direct-methods program system *MULTAN* (Main, Fiske, Hull, Lessinger, Germain, Declercq & Woolfson, 1980) was applied to the contributions to the structure factors of the Fe atoms as determined by our procedure. The data sets without error and with $\sigma = 4\%$ were used. E maps computed with the phases from the sets of second-highest combined FOM (by the very nature of our procedure the ψ zero criterion cannot be used) clearly reveal all Fe atoms, both for $\sigma = 0$ and $\sigma = 4\%$.

Table 2. *Average values* $\langle |X - Xe| \rangle$ *for the bianomalous (bia) and* $\langle |T - Te| \rangle$ *for the monoanomalous (mon) cases at given* λ *and* σ *values*

		σ			
	λ (Å)	0·01	0·02	0·04	
	1·54052	0·04	0·08	0·14	bia
	1·74300	0·02	0·04	0·08	bia
1·54052;	1·78892	0·04	0·07	0·15	mon

Table 3. *The bianomalous case: standard deviation* σ *of the error* (%), *number of reflections and* R_{F_0} *and* R_g *indices* (%) *for each family of reflections (see text for further details)*

Family of reflections	σ	Number of reflections	R_{F_0}	R_g
Non-centrosymmetric reflections	0	1371	0·1	3·0
	1	1384	0·2	12·0
	2	1382	0·3	21·9
	4	1345	0·5	36·6
Centrosymmetric reflections	0	784	0·1	2·9
	1	787	0·1	4·8
	2	786	0·1	7·2
	4	802	0·2	12·8
All reflections	0	2155	0·1	3·0
	1	2171	0·2	9·4
	2	2168	0·2	16·4
	4	2147	0·3	27·4

Table 4. *The monoanomalous case: standard deviation* σ *of the error* (%), *number of reflections and* R_g *index* (%) *for each family of reflections*

Family of reflections	σ	Number of reflections	R_g
Non-centrosymmetric reflections	0	1426	1·9
	1	1410	4·4
	2	1398	7·2
	4	1424	13·6
Centrosymmetric reflections	0	589	3·6
	1	578	6·4
	2	583	9·7
	4	577	16·4
All reflections	0	2015	2·4
	1	1988	5·0
	2	1981	8·0
	4	2001	14·5

Table 5. *The bianomalous case: standard deviation* σ *of the error* (%), *number of reflections and* R_{F_0} *and* R_g *indices* (%) *for each family of reflections (see text for further details)*

Family of reflections	σ	Number of reflections	R_{F_0}	R_g
Non-centrosymmetric reflections	0	986	0·2	3·0
	1	981	0·2	7·0
	2	985	0·3	11·4
	4	995	0·4	22·0
Centrosymmetric reflections	0	1005	0·1	5·4
	1	1008	0·1	6·5
	2	999	0·1	8·1
	4	1014	0·2	12·8
All reflections	0	1991	0·1	4·2
	1	1989	0·2	6·7
	2	1984	0·2	9·7
	4	2009	0·3	17·2

Table 6. *Fractional coordinates* ($\times 10^4$) *of the* Fe *atoms in ferredoxin*

For each atom the first line gives the coordinates as determined by Adman *et al.* (1972); the second and third lines give the results obtained by the two-wavelength technique applied to the data sets without error and with $\sigma = 4\%$ respectively.

	x	*y*	*z*
Fe(1)	5	2089	2957
	14	1994	3115
	7	2112	3023
Fe(2)	407	2523	3453
	400	2497	3390
	420	2502	3392
Fe(3)	9937	1936	3614
	9976	1940	3628
	9994	2023	3618
Fe(4)	9536	2537	3354
	9597	2497	3387
	9552	2504	3386
Fe(5)	8328	253	5142
	8336	209	5092
	8319	320	5140
Fe(6)	7546	166	4862
	7531	201	4998
	7549	292	4924
Fe(7)	7665	617	5402
	7856	721	5240
	7818	596	5320
Fe(8)	7906	776	4773
	7961	740	4771
	7898	746	4741

In Table 6 the coordinates of the highest eight peaks in these low-resolution E maps are compared with those determined by Adman *et al.* (1973). The mean difference appears to be only 0·2 Å.

7. Discussion

The technique that is used most for localizing anomalous scatterers is the difference-Patterson synthesis with coefficients $(|F_{\mathbf{h}}^{+}| - |F_{\mathbf{h}}^{-}|)^2$ as proposed by Rossmann (1961). The interpretation of such a single-wavelength anomalous-dispersion Patterson map is handicapped by the presence of a background. This may be remedied by combining anomalous-dispersion information with isomorphous-crystal data (Kartha & Parthasarathy, 1965).

The major merit of two-wavelength techniques is the fact that one need no longer be dependent on the existence of derivatives that exhibit a sufficiently high degree of isomorphism with the native compound for localizing the anomalous scatterers. Although various contributions to the two-wavelength approach have already been made, the expressions we give in the present paper are the first ones that permit straightforward calculation of the anomalous-scatterer contribution to the structure factor in the monoanomalous case as well as in the bianomalous case. Thus the location of the anomalous scatterers, even if they are relatively light, can be carried out; this is where conventional techniques, like the usual Patterson synthesis with observed intensities obviously fail. At the same time the anomalous-scatterer configuration determined by virtue of its calculated structure-factor contribution, serves to detect spurious anomalous effects, before they are used for phase determination.

The application of the formulae to the ferredoxin structure led to excellent results even when the data used were artificially contaminated with fairly large errors. An improvement of the accuracy might be attained when the procedure is extended to *multi*-wavelength experiments.

We wish to thank Dr H. A. Krabbendam for valuable discussions and Mr A. J. A. R. Blankensteijn for computational assistance.

References

ADMAN, E. T., SIEKER, L. C. & JENSEN, L. H. (1973). *J. Biol. Chem.* **248**, 3987–3996.

BARTUNIK, H. D. (1978). *Acta Cryst.* A**34**, 747–750.

DODSON, E. & VIJAYAN, M. (1971). *Acta Cryst.* B**27**, 2402–2411.

HOPPE, W. & JAKUBOWSKI, U. (1975). *Anomalous Scattering*, edited by S. RAMASESHAN & S. C. ABRAHAMS, pp. 437–461. Copenhagen: Munksgaard.

KARLE, J. (1980). Collected Abstracts, 6th European Crystallographic Meeting, p. 137.

KARTHA, G. & PARTHASARATHY, R. (1965). *Acta Cryst.* **18**, 745–749.

MAIN, P., FISKE, S., HULL, S. E., LESSINGER, L., GERMAIN, G., DECLERCQ, J. P. & WOOLFSON, M. M. (1980). *MULTAN. A System of Computer Programs for the Automatic Solution of Crystal Structures from X-ray Diffraction Data*. Univs. of York, England, and Louvain, Belgium.

MATTHEWS, B. W. (1966). *Acta Cryst.* **20**, 230–239.

PARTHASARATHY, S. (1967). *Acta Cryst.* **22**, 98–103.

PARTHASARATHY, S. & SRINIVASAN, R. (1964). *Acta Cryst.* **17**, 1400–1407.

PETSKO, G. A. (1976). *Acta Cryst.* A**32**, 473–476.

PHILLIPS, J. C., TEMPLETON, D. H., TEMPLETON, L. K. & HODGSON, K. O. (1978). *Science*, **201**, 257–259.

PHILLIPS, J. C., WLODAWER, A., GOODFELLOW, J. M., WATENPAUGH, K. D., SIEKER, L. C., JENSEN, L. H. & HODGSON, K. O. (1977). *Acta Cryst.* A**33**, 445–455.

RAMASESHAN, S. (1966). *Curr. Sci.* **35**, 87–91.

ROSSMANN, M. G. (1961). *Acta Cryst.* **14**, 383–388.

SIEKER, L. C., ADMAN, E. T. & JENSEN, L. H. (1972). *Nature (London)*, **235**, 40–42.

SINGH, A. K. & RAMASESHAN, S. (1968). *Acta Cryst.* B**24**, 35–39.

UNANGST, D., MÜLLER, E., MÜLLER, J. & KEINERT, B. (1967). *Acta Cryst.* **23**, 898–901.

WILSON, A. J. C. (1949). *Acta Cryst.* **2**, 318–321.